JOURNAL OF SPACECRAFT AND ROCKETS
Vol. 32, No. 3, May–June 1995

Oxygen Interactions with Materials III—Mission and Induced Environments

Steven L. Koontz,* Lubert J. Leger,† and Steven L. Rickman‡
NASA Johnson Space Center, Houston, Texas 77058
Charles L. Hakes§ and David T. Bui¶
Lockheed Engineering and Sciences Company, Inc., Houston, Texas 77058
Donald E. Hunton**
U.S. Air Force Phillips Laboratory, Hanscomb Air Force Base, Massachusetts 01731
and
Jon B. Cross††
Los Alamos National Laboratory, Los Alamos, New Mexico 87545

The Evaluation of Oxygen Interactions with Materials III (EOIM-III) flight experiment was developed to obtain benchmark atomic-oxygen–material reactivity data. The experiment was conducted during Space Shuttle mission 46, July 31 to August 7, 1992. Quantitative interpretation of the materials reactivity measurements requires a complete and accurate definition of the space environment exposure, including the thermal history of the payload, the solar ultraviolet exposure, the atomic-oxygen fluence, and any spacecraft outgassing and contamination effects. The thermal history of the payload was measured using 11 thermocouple sensors placed behind selected samples and on the EOIM-III payload structure. The solar ultraviolet exposure history of the EOIM-III payload was determined by analysis of the as-flown orbit and vehicle attitude combined with daily average solar ultraviolet and vacuum ultraviolet fluxes. The atomic-oxygen fluence was assessed in three ways. First, the O-atom fluence was calculated using a program that incorporates the MSIS-86 atmospheric model, the as-flown Space Shuttle trajectory, and solar activity parameters. Second, it was estimated directly from Kapton film erosion. Third, ambient O-atom measurements were made using the quadrupole mass spectrometer on the EOIM-III payload. As of this writing, our best estimate of the O-atom fluence is $(2.3 \pm 0.3) \times 10^{20}$ atoms/cm^2. Finally, results of postflight surface analysis of selected samples by x-ray photoelectron spectroscopy indicate low levels of molecular contamination on the payload surface.

Nomenclature

A_p = solar geomagnetic index
a = orbit angle
a_1 = terminator exit orbit angle
a_2 = orbit angle where blockage begins
F_{ACC} = accumulated direct solar flux
$F_{10.7}$ = solar electromagnetic emission at 10.7 cm
S = solar flux
α = solar absorptance
β = angle between the sun-Earth vector and the orbit plane (assumed constant over a single orbit)
ε = infrared emissivity

Introduction

PREVIOUS studies[1] of atomic-oxygen reactivity with materials used on spacecraft in low Earth orbit (LEO) have been based on changes in material properties measured in the laboratory and normalized to the atomic-oxygen fluence as derived from spacecraft flight conditions and ambient-density predictions (MSIS-86).[2,3] Some questions regarding the validity of using long-term-based ambient density models for short-term flight experiments have arisen.[4,5] To resolve this uncertainty and to test a wide variety of new materials for which no space-flight data were available, the Evaluation of Oxygen Interactions with Materials III (EOIM-III) flight experiment was conducted on Space Shuttle mission 46 (STS-46), which flew July 31 to August 7, 1992. This paper presents a detailed description of the space environment exposure for STS-46 and the EOIM-III flight experiment. An overview of EOIM-III flight measurements and supporting ground measurements is included in an accompanying paper.[6]

Flight Hardware

EOIM-III was mounted on a multipurpose payload and experiment support structure on the starboard side of the Space Shuttle Atlantis near the aft bulkhead and at the level of the orbiter still longeron (that is, at the level of the cargo-bay door hinge line) as shown in Figs. 1 and 2. The carousel and mass spectrometer are visible in the middle of the EOIM-III pallet, with the passive sample carriers on the outboard side and the heated trays and environmental monitor package inboard, toward the center of the Space Shuttle cargo bay. The mass-spectrometer ion source was of the semiopen variety as defined by Hayden et al.[7] and was capable of receiving neutral gas from a 180-deg field of view. Only the vertical stabilizer, several cargo-bay components including the aft bulkhead, and the orbital maneuvering system pods are line-of-sight to the mass-spectrometer ion source (although occupying only a small, peripheral fraction of the field of view) and, by implication, the rest of the payload. A cross-sectional drawing of the mass spectrometer is shown in Fig. 2.

Flight Summary

The STS-46 mission altitudes and attitudes were scheduled to accommodate three primary payloads, of which the EOIM-III was the third and final. The orbital inclination was 28.5 deg, and the solar β

Received March 22, 1994; revision received Oct. 20, 1994; accepted for publication Oct. 26, 1994.

*Materials Engineer.
†Branch Chief, Materials. Associate Fellow AIAA.
‡Aerospace Engineer.
§Principal Scientist, 2400 NASA Road 1. Member AIAA.
¶Engineer, 2400 NASA Road 1.
**Scientist, Ionospheric Physics Branch. Member AIAA.
††Senior Scientist, Chemical Physics Division. Member AIAA.

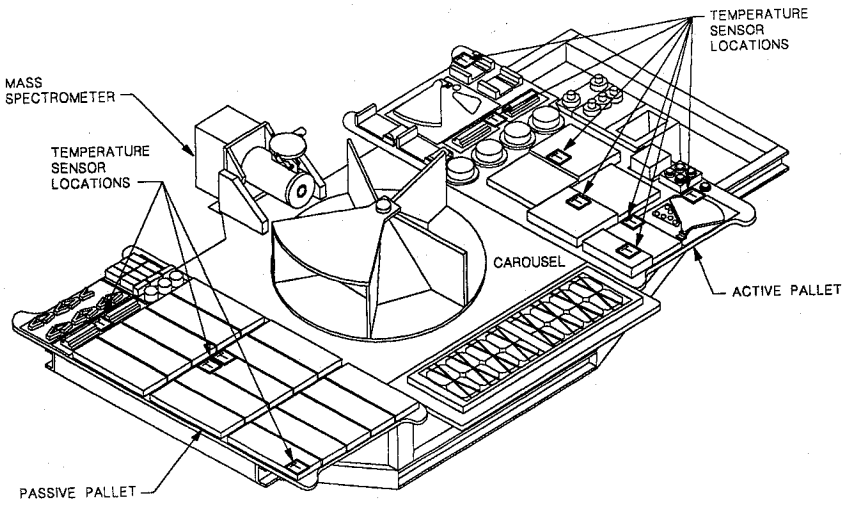

Fig. 1a EOIM-III payload configuration with temperature sensor locations (marked with a boxed T).

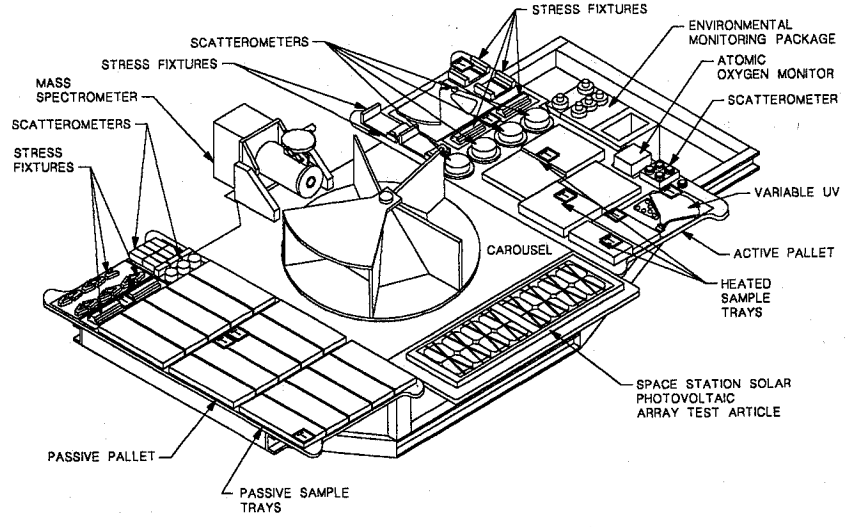

Fig. 1b EOIM-III subexperiment locations.

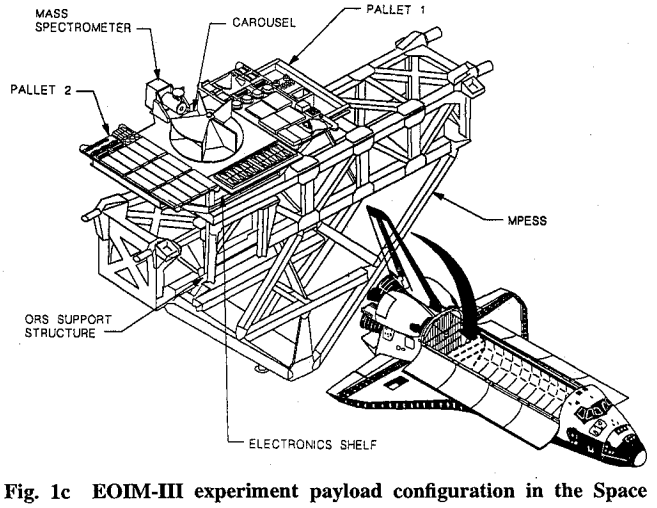

Fig. 1c EOIM-III experiment payload configuration in the Space Shuttle cargo bay.

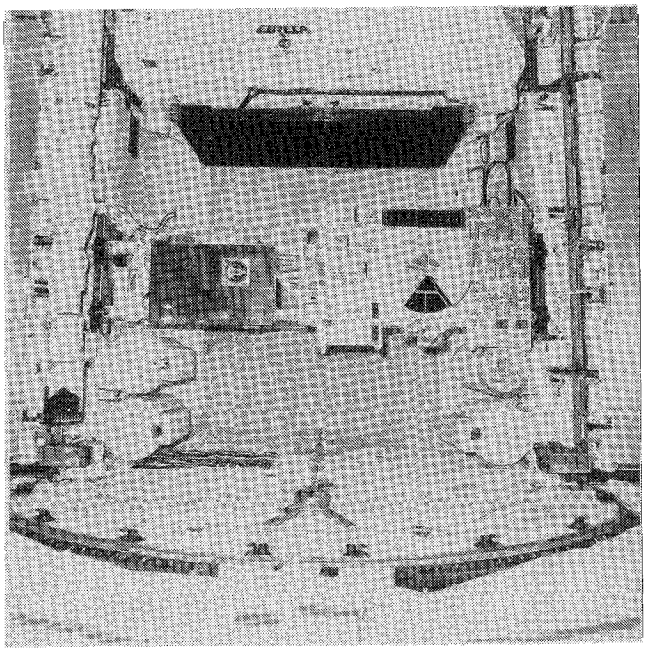

Fig. 2 EOIM-III experiment as installed in Space Shuttle cargo bay before launch.

angle (the angle between the orbit plane and the Earth-sun vector) varied between 17.5 and 24.3 deg. The STS-46 flew three altitudes. The highest (430 km) orbit, occurring from MET (mission elapsed time) 0 to 70 h, was flown to support the release of the EURECA (European Retrievable Carrier) satellite. The second (300 km) orbit, occurring from MET 70 to 140 h, was for Tethered Satellite System operations. The lowest (230 km) orbit supported the EOIM-III

experiment, exposing the orbiter and all payloads to a far denser atmosphere than the earlier, higher orbits. The molecular density of the atmosphere at the EOIM-III altitude was approximately 10 times higher than the density at the tethered-satellite deployment altitude, and approximately 100 times higher than the EURECA-release altitude. Because of the density increase at low altitudes and the nonram orientations flown during most of the rest of the flight, approximately 95% of the total atomic-oxygen fluence occurred during the EOIM-III portion of the mission.

The environmental exposure of the EOIM III payload also depended on the attitude of the orbiter with respect to the direction of flight (ram direction) and with respect to the Sun. The attitude timeline in Fig. 3 shows the ram angle, the angle between the cargo-bay normal ($-Z$ in Space Shuttle orbiter body coordinates), and the orbiter velocity vector (VV). The ram angle shown runs from 0 deg, corresponding to the $-Z$ VV or ram orientation, to 180 deg, corresponding to Z VV or antiram (heat shield into the VV). The oscillations between 0 and 180 deg visible during earlier parts of the mission correspond to various inertial hold attitudes or roll maneuvers. The EURECA-release portion of the flight included periods of ram attitude and periods of a solar inertial hold, during which time the cargo bay was facing the sun. The EOIM-III mass spectrometer was on for approximately 17 h during this part of the flight. During deployment of the tethered-satellite system, the flight attitude was mostly an "airplane mode" orientation—the cargo bay was facing away from Earth. The mass spectrometer was on for about 4 h during tethered-satellite operations.

EOIM-III was initiated at MET 5 days, 22 h, 30 min (5:22:30 = 142.5 h) shortly after reducing orbital altitude to 123–124 n.mi. A wastewater dump was conducted between MET 5:20:37 and MET 5:22:30 with the Space Shuttle attitude adjusted to minimize the chance of particles from the waste stream recontracting the Space Shuttle. The Space Shuttle was placed in the $-Z$ VV attitude for EOIM-III at MET = 142.5 h.

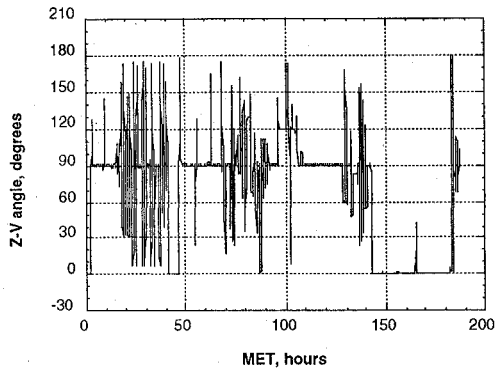

Fig. 3 STS-46 mission attitude timeline.

Thermal History

The thermal history of the EOIM-III payload was measured by 11 thermocouple sensors placed behind selected samples and on the EOIM-III payload structure (Fig. 1a). Because of noise in the temperature data and the large number of measurements from each sensor (one sample per second), the data were appropriately filtered and time-averaged before plotting. Figures 4a through 4d show the filtered output of selected sensors. Temperature variations are consistent with vehicle flight conditions, with the hottest period for the passive plates occurring during the EURECA release. Diurnal variations in temperature are visible in the data (note MET 100–130 h on the figures). Other temperature variations are due to vehicle attitude or operation of heaters on the temperature-controlled plates.

The thermal mass, thermal conductivity, and thermal-radiative properties α (solar absorptance) and ε (infrared emissivity) of the thermocouple mounting assembly determine the temperature reported by a thermocouple sensor. This temperature is only an approximation of the temperature of any nearby materials samples.The effects of sample thermo-optical property variations can be gauged by a comparison of the two thermocouple readings from the passive pallet sample disk carrier 8 sample cells shown in Figs. 4a and 4b. The physical configurations of the two thermocouple sensors were identical, except for sample thermo-optical properties, and the sensor assemblies were adjacent to each other on the sample carrier

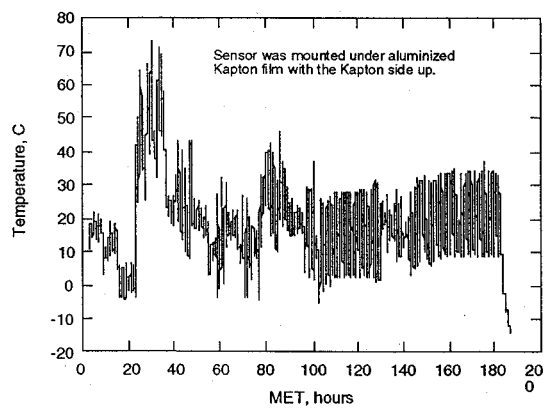

Fig. 4a Passive pallet sample disk/carrier.

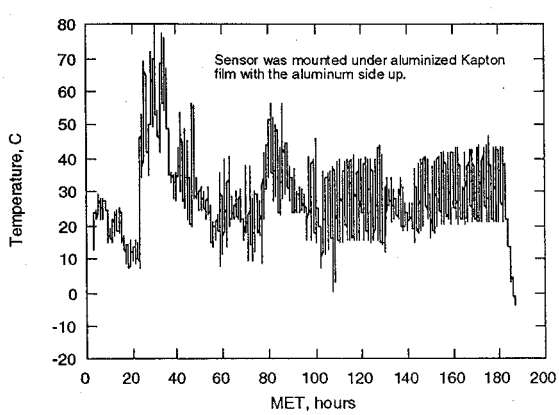

Fig. 4b Passive pallet sample disk/carrier.

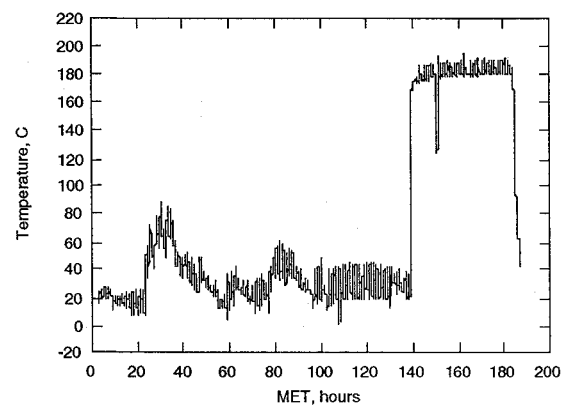

Fig. 4c Active pallet (200°C) heated plate at the sample disk.

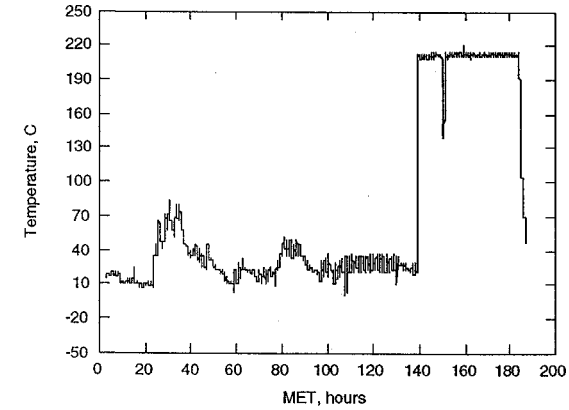

Fig. 4d Active pallet (200°C) heated plate at the thermostat.

(adjacent sample cells). The thermo-optical properties were determined by the choice of sample material mounted on top of each sensor: aluminized Kapton film with the aluminum side up in one case ($\alpha = 0.12, \varepsilon = 0.04, \alpha/\varepsilon = 3$) (Fig. 4b) and the Kapton side up in the other ($\alpha = 0.33, \varepsilon = 0.82, \alpha/\varepsilon = 0.4$) (Fig. 4a). The effect of the large difference in α/ε can be seen in Figs. 4a and 4b, where the aluminum-side-up sensor shows significantly higher temperatures throughout the mission. During the 42-h EOIM-III period, the average temperatures were 303.6 and 293.0 K for the aluminum-side-up sensor and the Kapton-side-up sensor, respectively. The extremes of temperature resulting from diurnal variations in solar heating were from 289.5 to 320.0 K for the aluminum-side-up sensor and from 278.3 to 309.9 K for the Kapton-side-up sensor.

Thermocouple sensors on the 473-K heated tray were placed both on the tray thermostat and in a sample-holder cell. The thermo-optical properties for the sample-cell sensor were determined with an anodized aluminum disk that was identical to the rest of the payload aluminum, so that any differences between the sensor readings were due to configuration interactions alone. The thermostat sensor on the 473-K tray shows a much smaller diurnal temperature variation and a significantly higher mean temperature than the sample-cell sensor (Figs. 4c and 4d). The mean, maximum, and minimum temperatures during the EOIM-III exposure (excluding the large temperature drop that occurred when the heater was off near MET 150 h) were 485.0, 488.1, 483.2 K for the thermostat sensor and 456.7, 464.7, 452.3 K for the sample-cell sensor.

The temperature measurements reported above were made to support definition of the sample temperature, as well as the uncertainty in sample temperature, both before and during the EOIM-III atomic-oxygen exposure. Measurements of sample-holder and payload-structure temperature provide only a first estimate of the actual sample temperature, which is also affected by the sample α/ε. The temperature measurements reported above show that average samples temperatures achieved during EOIM-III were within 5% of the design temperature even in the presence of large variations in sample α/ε. The average temperatures reported by thermocouple sensors on various EOIM-III subexperiments during the ram oxygen exposure are shown in Table 1. The uncertainty in the corresponding sample temperatures is estimated at 5% of the indicated value.

Solar Ultraviolet and Vacuum Ultraviolet Exposure

An analytical determination of the equivalent sun hours (the energy received by a surface with the sun normally incident to it for 1 h) experienced by the EOIM-III payload was performed to determine the solar ultraviolet and vacuum ultraviolet (uv-vuv) doses to exposed materials. EOIM-III operations consisted of only a few attitudes. Prior to EOIM-III operations, however, numerous attitudes were flown. Hence, two different methods were used to calculate the solar exposure.

The Thermal Interactive Mission Evaluation System (TIMES89)[8] computer program was used to characterize the solar exposure in the period prior to EOIM-III experiment operations. This program allows analysis of unshadowed sensing surfaces as they move and reorient throughout their orbit. The solar irradiance on the experiment was calculated using the as-flown mission attitude timeline and the known orbit parameters. While all major attitudes were analyzed (both local-vertical local-horizontal and inertially referenced), simplifying assumptions in the TIMES89 code prohibit modeling of attitude-to-attitude transitions. Thus, exposure during these periods was approximated by holding the previous attitude until halfway through the transition period and then instantaneously switching to the new attitude. The assumption of unshadowed sample surface should hold reasonably well for this configuration, as the sun sensor was located high in the cargo bay and had few potential solar-illumination blockers.

For the period of time encompassing EOIM-III operations, the cargo bay was facing into the velocity vector direction; and the majority of the time was spent in either a tail-to-Earth or a nose-to-Earth attitude. Since this period of time was of specific interest, a more detailed assessment of the potential blockage by orbiter components was performed. A detailed geometric model of the configuration was used, and the location of the onset of solar blockage was assessed based on line-of-sight considerations using the thermal synthesizer system (TSS) software.[9] These data were used in conjunction with the following equation to determine the accumulated solar flux (F_{ACC}) during each orbit:

$$F_{ACC} = S \cos\beta \int_{a_1}^{a_2} (-\sin a)\, da = S \cos\beta \, [\cos a]_{a_1}^{a_2} \qquad (1)$$

Note that this equation applies only to the case where the orbiter cargo bay faces into the velocity vector direction. Also, for all locations other than between the orbit angles a_1 and a_2, $F_{ACC} = 0$ because of blockage or angles greater than 90 deg with respect to the solar vector.

If the accumulated direct solar flux is divided by the product of the solar constant and the orbit period, the result is the equivalent sun hours for that orbit. The solar uv exposure is calculated by multiplying the equivalent sun hours by the uv-vuv fluxes measured by the Solar-Stellar Comparison Experiment 1 (SOLSTICE)[10–12] on the Upper Atmosphere Research Satellite (UARS). The resulting solar uv exposure values are presented in Tables 2 and 3. Note that the short-wavelength limit for SOLSTICE is 119 nm, so the values in the interval 119 to 10 nm are not measurements, but are from a model that uses the solar 10.7-cm radio flux.[13] The 1-σ uncertainty for UARS measurements is 5%, and for the extreme ultraviolet model results is 30%.

Atomic-Oxygen Fluence

The atomic-oxygen fluence is determined in three ways. First, the AOFLUX (atomic-oxygen fluence) computer program, which incorporates the MSIS-86 atmospheric model and the as-flown Space Shuttle trajectory, was used. Second, the fluence measured

Table 1 Average temperatures of EOIM-III subexperiments

Thermocouple location	Average temperature, K
Passive tray, Kapton/Al sample	294
Passive tray, Al/Kapton sample	304
Heated tray, 333 K, Al sample	337
Heated tray, 393 K, Al sample	392
Heated tray 473 K, Al sample	456
Static stress fixture (MSFC)	293
Composite stress fixture, pallet 1	294
Composite stress fixture, pallet 2	289

Table 2 Solar ultraviolet spectral irradiance history

Mission days[a]	Sun hours	Irradiance, mW/cm^2				
		λ = 250–200 nm	200–150 nm	150–119 nm	121.5 nm	119–10 nm
0–2.0	5.8	2.00×10^{-1}	9.82×10^{-3}	1.10×10^{-3}	8.81×10^{-4}	3.4×10^{-4}
2.0–4.0	6.8	2.01×10^{-1}	9.85×10^{-3}	1.13×10^{-3}	9.10×10^{-4}	3.6×10^{-4}
4.0–5.8	10.4	2.01×10^{-1}	9.89×10^{-3}	1.16×10^{-3}	9.31×10^{-4}	3.7×10^{-4}
5.8–6.0[b]	0.5	2.02×10^{-1}	9.93×10^{-3}	1.17×10^{-3}	9.45×10^{-4}	3.7×10^{-4}
6.0–7.0[b]	4.4	2.02×10^{-1}	9.95×10^{-3}	1.18×10^{-3}	9.51×10^{-4}	3.8×10^{-4}
7.0–8.0[b]	3.0	2.02×10^{-1}	9.99×10^{-3}	1.19×10^{-3}	9.63×10^{-4}	3.8×10^{-4}

[a]MET. The numbers shown represent the beginning time and time of the measurement interval in days.
[b]EOIM-III exposure period.

Table 3 Cumulative solar ultraviolet spectral incidence

Wavelength, nm	Cumulative incidence, J/cm^2
250–200	22.4
200–150	1.10
150–119	0.128
121.5	0.103
119–10	0.04

directly from Kapton film erosion. Such measurements are discussed in detail in Ref. 6. Finally, ambient oxygen-atom measurements were made using a mass spectrometer that was calibrated before and after the mission in the HVAB (high-velocity neutral-atom beam) system at the LANL (Los Alamos National Laboratory).[14] All fluence estimates are summarized in Table 4. As shown there, the MSIS-86 calculations, mass-spectrometer measurements, and Kapton weight-loss or profilometry measurements produce nearly identical fluence determinations.

AOFLUX Calculations

The AOFLUX program, written to calculate the expected O-atom fluence, was based on the MSIS-86 atmospheric model[2,3] and the as-flown timeline (which included the altitude, latitude, and longitude). Solar activity parameters recorded during STS-46 at the Space Environment Services Center (National Oceanic and Atmospheric Administration) were used (instead of monthly average values) to allow for the magnetic substorm activity observed during EOIM-III. Mission-specific values for the daily-average geomagnatic activity A_p and the daily solar radio noise flux values $F_{10.7}$ are given in Table 5.[15]

The O-atom densities calculated from MSIS-86 were used with the velocity of the spacecraft to calculate the total flux to the spacecraft. Integrating the total flux throughout the mission gives a total fluence to the spacecraft (before orientation effects are included) of 3.4×10^{20} O atoms/cm^2. The total flux at each time increment was multiplied by the cosine of the ram angle (shown in Fig. 3) to obtain the net flux to the EOIM-III payload (shown in Fig. 5). Note that the fluxes for angles greater than 90 deg were simply set to zero. By integrating the net flux throughout the mission, the fluence to the EOIM-III payload is calculated to be 2.3×10^{20} O atoms/cm^2 (Table 4). Of this net fluence, 95% occurs during the low-altitude ram orientation (Fig. 5). The magnitude of the diurnal variations during the ram period between hours 142 and 185 can also be seen in the figure.

Kapton Recession Measurements

Measurements of Kapton polyimide surface recession or weight loss made following several previous LEO flight experiments[4,16,17] have produced the widely accepted value of the Kapton reaction efficiency of $(3.0 \pm 0.3) \times 10^{-24}$ cm^3/atom. MSIS-86 was used to calculate the O-atom fluence needed to calculate polymer reaction efficiencies in all previous LEO flight experiments. To determine the EOIM-III O-atom fluence using Kapton surface recession or weight-loss measurements, without referring indirectly to MSIS-86 calculations, an independent measurement of Kapton reaction efficiency was conducted in the HVAB at LANL (described in Ref. 6). The EOIM-III O-atom fluence based on the LANL measurement of the Kapton polyimide reaction efficiency is $(2.3 \pm 0.07) \times 10^{20}$ atoms/cm^2 based on weight loss and $(2.4 \pm 0.09) \times 10^{20}$ O-atoms/cm^2 based on surface recession measured by profilometry.

Mass-Spectrometer Measurements

The EOIM-III quadrupole ion neutral mass spectrometer[18] scanned a mass-to-charge ratio range of 0 to 72 amu/e every 5.12 s with a digital resolution of 0.142 (amu/e) channel (512 digital data channels corresponding to 0–72 amu/e). The mass-spectrometer resolution $\Delta M/M$, calculated as the mass peak width (full width at half maximum) at mass 28, was 0.011 throughout the mission and during the preflight and postflight calibrations. The mass-spectrometer output signal was logarithmically amplified, which permitted the display of seven orders of magnitude in mass-spectrometer detector current in a 0- to 5-V analog signal that was then digitized with an 8-bit analog-to-digital converter. Mass spectra were produced in either ion or neutral operating mode. In neutral mode, a repeller grid excluded naturally occurring ionospheric ions, and neutral gaseous species entering the ion source were ionized by electron impact. In ion mode, the repeller grid and the filaments producing electrons for electron impact ionization were shut off, and naturally occurring ionospheric ions entering the ion-source volume were mass-analyzed and detected.

The primary objective of the EOIM-III mass-spectrometer experiment was to measure the O-atom fluence for comparison with the fluence calculated using the MSIS-86 model of the thermosphere. The mass spectrometer was subjected to an extensive calibration process both before and after the flight (as described in an accompanying paper[14]) to permit accurate quantitative estimates of O-atom flux and fluence from the mass-spectrometer data. The O-atom fluence was determined as follows. First, the data were divided into 5-min intervals corresponding to the 5-min intervals used in the MSIS-86 calculations. Within each interval, all complete, valid spectra appropriate for use in neutral flux and fluence calculations were averaged. A typical 5-min-average spectrum taken early in the

Table 4 Summary of EOIM-III atomic oxygen fluence estimates

Measurement method	Fluence	Measurement uncertainty
AOFLUX (MSIS-86) calculation	2.3×10^{20}	$\pm 0.35 \times 10^{20}$ [a]
Kapton erosion weight loss (3 samples)	2.34×10^{20}	$\pm 0.07 \times 10^{20}$ [b]
Kapton erosion profilometry (4 samples)	2.41×10^{20}	$\pm 0.09 \times 10^{20}$ [c]
Mass spectrometer—empirical calibration from in-flight data	2.3×10^{20}	$\pm 0.14 \times 10^{20}$

[a] 15% estimated from MSIS.
[b] Weight-loss uncertainty.
[c] Profilometry uncertainty.

Table 5 Daily-average geomagnetic activity values A_p and daily solar $F_{10.7}$

Date	Daily A_p	Daily $F_{10.7}$	90-day average $F_{10.7}$
07/31/1992	11	103.0	125.0
08/01/1992	09	110.0	125.0
08/02/1992	06	125.0	124.0
08/03/1992	05	131.0	124.0
08/04/1992	13	131.0	124.0
08/05/1992	43	131.0	124.0
08/06/1992	19	138.0	124.0
08/07/1992	42	141.0	125.0
08/08/1992	22	144.0	125.0

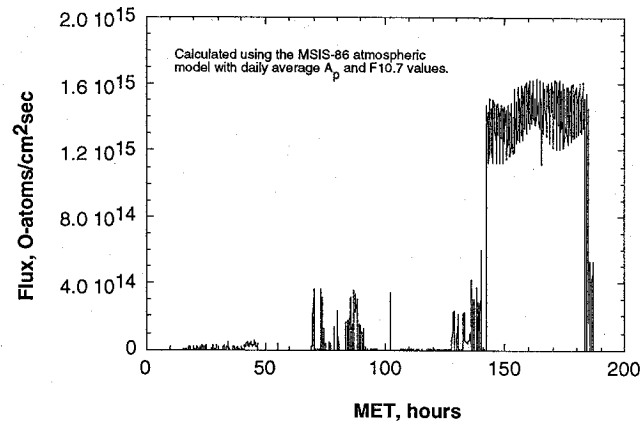

Fig. 5 Atomic-oxygen flux on the EOIM-III payload during STS-46 as calculated with MSIS-86.

EOIM-III ram exposure period is shown in Fig. 6. Figure 7 shows an overview of the 5-min-average spectra taken throughout STS-46. The data have been averaged into 1-h time blocks for a qualitative view of the entire STS-46 mission. The start of the mission is toward the front of the picture, and flat lines indicate the times when the mass spectrometer was either turned off, facing the carousel, or in ion mode.

The 5-min-average spectra were used to calculate the O-atom fluence. Mass peak areas (peak sums), not peak heights, were used throughout to obtain the best possible signal-to-noise ratio. Peak sums, which retained the units of amperes, were calculated by summing the mass-spectrometer signal amplitude in the seven adjacent digital data channels containing a mass peak. The unmodified peak sums for the $M/e = 16$, 28, and 32 peaks (O, N_2, and O_2) are shown in Figs. 8–10. To calculate the O-atom flux, the peak sum at $M/e = 16$ was corrected for contributions from $M/e = 16$ fragment ions from molecular oxygen and water by subtracting 26% of the $M/e = 32$ (O_2) peak sum and 1.7% of the $M/e = 18$ (H_2O) peak sum, as determined during preflight and postflight calibrations at LANL. The O-atom flux that produced each 5-min-average spectrum was then calculated by multiplying the corrected $M/e = 16$ peak sum by a calibration function described below. The net O-atom fluence was then determined by adding up the fluences for the various 5-min periods. The result is summarized in Fig. 11.

The calibration function was derived from both ground-based calibration of the mass spectrometer in the HVAB at LANL and mass-spectrometer performance data from STS-46. The EOIM-III mass spectrometer showed an O-atom-fluence-dependent sensitivity decay both in the HVAB at LANL and during STS-46.[14] However, different sensitivity decay functions were observed in the lab and on orbit (Fig. 12). For this resion, the zero-fluence O-atom flux calibration factor determined in the HVAB at LANL was used with

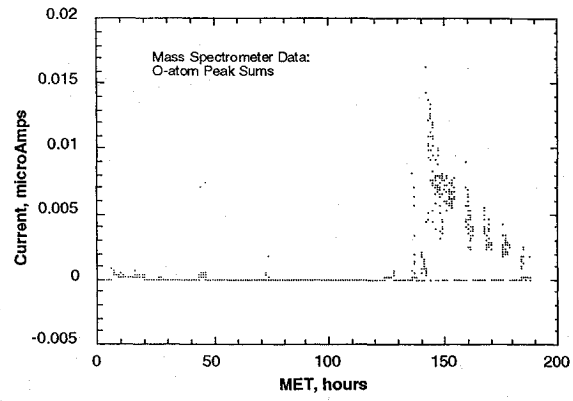

Fig. 8 O-atom ($e/M = 16$) current.

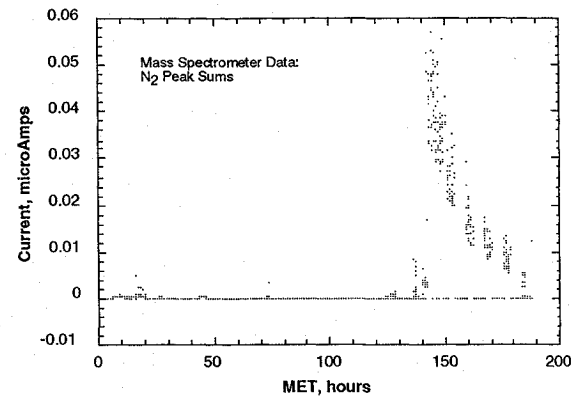

Fig. 9 N_2 ($e/M = 28$) current.

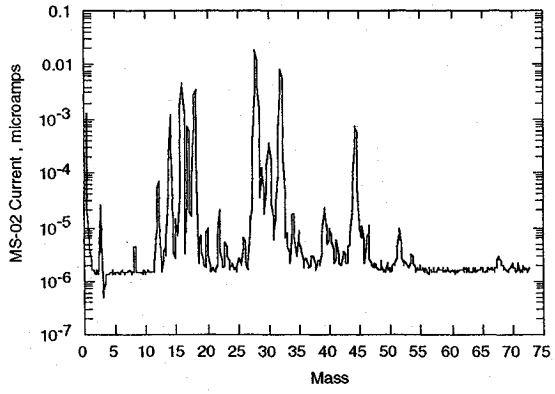

Fig. 6 A typical 5-min-average neutral mass spectrum from the early part of the low-altitude ram period.

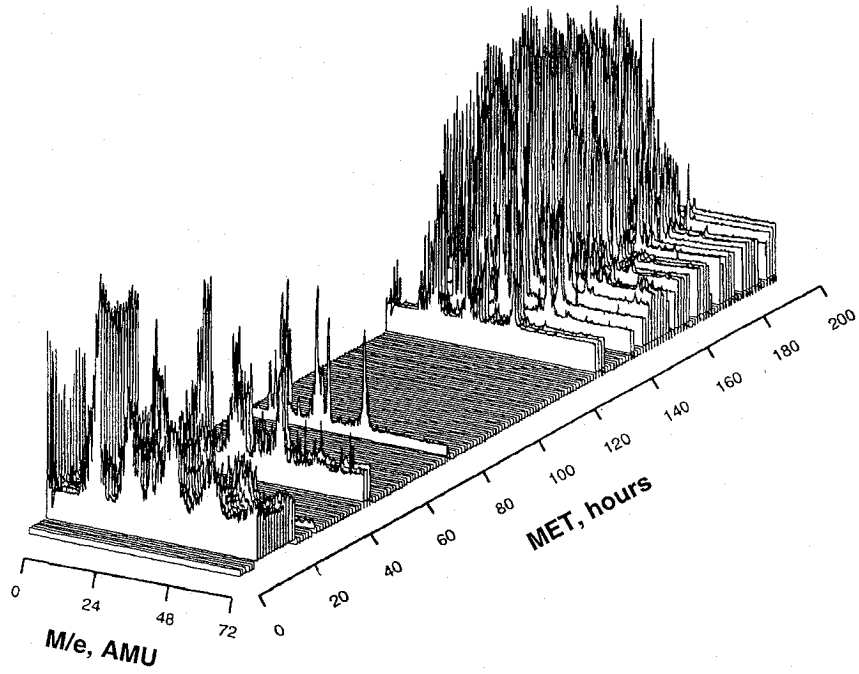

Fig. 7 An overview of the neutral spectra from the EOIM-III mass spectrometer from STS-46.

an empirical sensitivity decay function derived from a fit to the corrected $M/e = 16$ peak sum data from STS-46 to produce the calibration function:

$$y = \frac{0.006}{0.0047968 - 0.0022472\ \log(\text{MET} - 142.5)} \quad (2)$$

Using this calibration function, the corrected O-atom peak sums, and the percentage of mass-spectrometer on-time, the measured EOIM-III mission fluence is $(2.3 \pm 0.14) \times 10^{20}$ O atoms/cm^2.

The EOIM-III mass spectrometer was calibrated for direct measurement of high-velocity O-atom flux both before and after flight on STS-46 in the HVAB at LANL. Details of the calibration methodology and a summary of calibration methods and results have been reported.[14] Calibration studies were conducted over a period of several years prior to STS-46 as well as after the mission. In general, the EOIM-III mass spectrometer showed excellent stability, with the O-atom flux at low O-atom fluence showing a maximum variation of 5% and the partial-pressure sensitivity factor for nitrogen gas varying by less than 10%. However, the apparent fragmentation yield of O^+ from O_2^+ was re-examined so that the previously reported 10% correction factor[14] was increased to 26% for O-atom fluence calculations as a result of thermal-gas calibration measurements conducted prior to and just after STS-46.[14] Mass-spectrometer performance and flight data are discussed at greater length in the accompanying papers.[14,6]

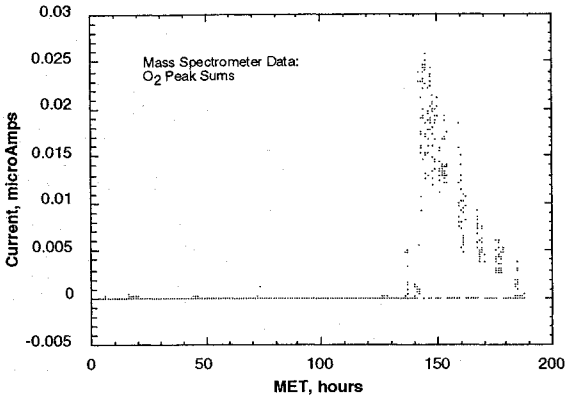

Fig. 10 O_2 ($e/M = 32$) current.

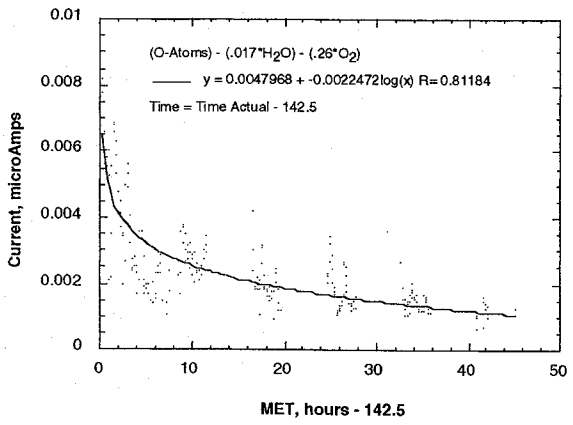

Fig. 11 Logarithmic fit to the corrected O-atom peak as a function of MET after 142.5 h.

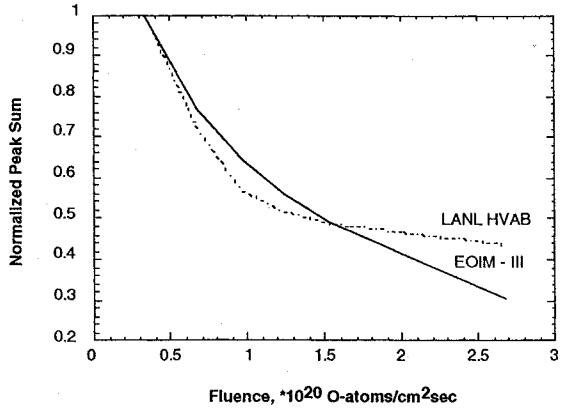

Fig. 12 Comparison of O-atom peak decay during flight and laboratory exposure.

EOIM-III Contamination

Since atomic-oxygen effects are influenced by contamination, deposits on sample surfaces were measured both in flight and after. In-flight measurements were made using quartz crystal microbalances (QCMs) in the Environment Monitor Package (EMP) provided by Goddard Spaceflight Center.[19] The EMP contained five QCMs—four coated with reactive materials and one not overcoated—and was located to the side of pallet 1 as shown on the right in Fig. 1a. The response from the uncoated crystal for the entire mission is shown in Fig. 13 and is representative of the response of all five microbalances. A large amount of contamination (several thousand angstroms) is indicated, and most of the deposition occurs during the EOIM-III portion of flight; contamination deposition is associated with ram atomic-oxygen exposure. Because of the inconsistency of these results with the numerous postflight x-ray photoelectron spectroscopy (XPS) surface analyses, which show only small amounts of contamination on the top plates of the experiment, it is expected that the EMP was contaminated from a localized source below the pallet top but within the EOIM-III hardware.

The results of the postflight contamination survey of the EOIM-III payload are shown in Table 6. XPS was used to measure the elemental composition and state of chemical combination of the near-surface region (10–50 Å from the surface) of the sample. Samples were surveyed for a variety of elements, but only silicon was identified as different from the substrate composition and is reported in Table 6. For all the surfaces measured, the substrate elements were evident in the XPS spectra, indicating incomplete coverage (less than 20 Å) of the contaminant layer. From the XPS results, it can be concluded that a small amount of contamination did deposit on the experiment pallets, but it is insignificant and should not affect the atomic-oxygen measurements.

Additional evidence confirms the relatively low levels of contamination occurring on EOIM-III samples: the measured reaction efficiencies of Kapton and other polymer films [which were in good agreement with measurements made on STS-8, STS-41, and LDEF (Long Duration Exposure Facility)], and the performance of the atomic-oxygen monitors (AOMs).[20] The AOMs consist of an array of thin-film carbon resistors, which showed increasing resistance as the carbon was removed by O-atom reaction. The AOMs showed a constant or slightly increasing rate of resistance change throughout the EOIM-III ram period, which would not be observed if a coating of SiO_2 were accumulating on the carbon resistor surfaces at the rates indicated by the EMP.

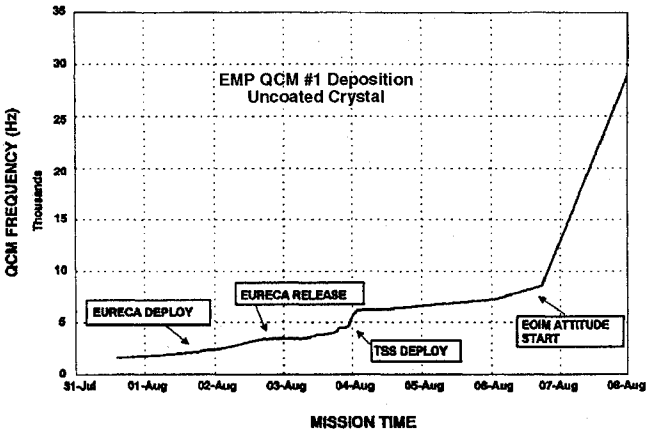

Fig. 13 Frequency change of uncoated crystal during the flight.

Table 6 Survey of EOIM-III x-ray photoelectron spectroscopy contamination

Payload location	Sample type	Si at. %
Mass-spec. ram	Silver/Teflon®	4.4
Mass-spec. payload bay view	Silver/Teflon	12.2
Mass-spec. starboard	Silver/Teflon	0.0
Mass-spec. ram	Kapton tape (exposed)	3.2
Mass-spec. ram	Kapton tape (unexposed)	0.0
Variable exposure tray mount	Steel washer (exposed)	2.7
Solar ultraviolet mount	Steel washer (exposed)	0.0
60°C tray	Steel ground strap	3.8
	Polysulfone (exposed)	0.8
	Polysulfone (unexposed)	0.0
	Mylar-A (exposed)	2.4
	Mylar-A (unexposed)	0.0
	Aluminum	7.1
120°C tray	Steel washer	7.7
	Kapton (exposed)	2.0
	Kapton (unexposed)	0.0
	Aluminum	9.4
	Aluminum	6.6
Passive trays 7, 8	7 polymer films	3.8 ± 2.6

Conclusions

A detailed characterization of the EOIM-III materials exposure environment has been completed. The atomic-oxygen fluence calculated using the MSIS-86 model of the thermosphere and as-flown Space Shuttle trajectory data (combined with the daily measurements of the solar activity and geomagnetic indices) is in good agreement with mass spectrometer and O-atom dosimeter measurements made during STS-46. Temperature measurements made during EOIM-III provide a complete thermal history of the payload and provide the investigators with useful sample temperature histories. UARS investigators provided solar uv and vuv measurements, which, combined with the STS-46 trajectory and vehicle attitude data, allow calculation of net solar uv and vuv radiation doses to the EOIM-III materials samples. Postflight XPS analysis of materials samples and in-flight performance of the AOM demonstrate that contamination of EOIM-III was, in fact, nominal and in no way interfered with the scientific and programmatic objectives of the payload. The severe contamination indicated by the TQCM (temperature-controlled quartz crystal microbalance) sensors in the EMP component of EOIM-III was localized in the immediate vicinity of the EMP.

Acknowledgments

We wish to thank Dennis Marton, University of Houston Chemistry Department, and Orlando Melendez, NASA Kennedy Space Center, for x-ray photoelectron spectroscopic measurements of EOIM-III samples.

References

[1]Visentine, J. T., and Leger, L. J., "Material Interaction with the Low Earth Orbital Environment: Accurate Reaction Rate Measurements," *Proceedings of the NASA Workshop on Atomic Oxygen Effects,* edited by D. E. Brinza, Jet Propulsion Lab., Publication 84-14, 1987, pp. 11–20.

[2]Heddin, A. E., "MSIS-86 Thermospheric Model," *J. Geophys. Res.*, Vol. 92, No. A5, 1987, pp. 4649–4662.

[3]Heddin, A. E., "High Altitude Atmospheric Modeling," NASA TM 100707, Oct. 1988.

[4]Visentine, J. T., Leger, L. J., Kuminecz, J. F., and Spiker, I. K., "STS-8 Atomic Oxygen Effects Experiment," AIAA Paper 85-0415, Jan. 1985.

[5]Visentine, J. T., and Leger, L. J., "Materials Interactions with the Low-Earth Orbital Environment: Accurate Reaction Rate Measurements," AIAA Paper 85-7019, Nov. 1985.

[6]Koontz, S. L., Leger, L. J., Visentine, J. T., Hunton, D. E., Cross, J. B., and Hakes, C. L., "EOIM-III Mass Spectrometry and Polymer Chemistry: STS 46, July–August 1992," *Journal of Spacecraft and Rockets*, Vol. 32, No. 3, 1995, pp. 483–495.

[7]Hayden, L. J., Nier, A. O., French, J. B., Reid, N. M., and Ducket, R. J., "The Characteristics of an Open Source Mass Spectrometer under Conditions Simulating Upper Atmosphere Flight," *International Journal of Mass Spectrometry and Ion Physics*, Vol. 15, 1974, pp. 37–47.

[8]Rickman, S. L., and Ortiz, C. R., "Thermal Interactive Mission Evaluation System (TIMES89)," NASA JSC-23852, Sept. 1989.

[9]Anon., *Thermal Synthesizer System (TSS) Users Manual LMSC/F191409,* Johnson Space Center (developed under contract NAS9-17923), Dec. 1992.

[10]Rottman, G. J., and Woods, T. N., High Altitude Observatory, National Center for Atmospheric Research, private communication to Steve Koontz.

[11]Rottman, G. J., Woods, T. N., and Sparn, T. P., "Solar-Stellar Irradiance Comparison Experiment 1: 1. Instrument Design and Operation," *Journal of Geophysical Research*, Vol. 98, No. D6, 1993, p. 10667.

[12]Woods, T. N., Rottman, G. J., and Ucker, G. J., "Solar-Stellar Irradiance Comparison Experiment 1: 2. Instrument Calibrations," *Journal of Geophysical Research*, Vol. 98, No. D6, 1993, p. 10679.

[13]Hinteregger, H. E., and Fukui, K., "Observational, Reference and Model Data on Solar EUV from Measurements on AE-E," *Geophysical Research Letters*, Vol. 8, No. 11, 1981, p. 1147.

[14]Cross, J. B., Koontz, S. L., and Hunton, D. E., "Flight Mass-Spectrometer Calibration in a High-Velocity Atomic-Oxygen Beam," *Journal of Spacecraft and Rockets*, Vol. 32, No. 3, 1995, pp. 496–501.

[15]Anon., Space Environment Services Center, Mission-specific values for the daily-average A_p geomagnetic activity and the daily solar $F_{10.7}$ values, private communication to Steve Koontz.

[16]Zimcik, D. G., and Magg, C. R., "Results of Apparent Oxygen Reactions with Spacecraft Materials During Shuttle Flight STS-41-G," *Journal of Spacecraft and Rockets*, Vol. 25, No. 2, 1988, pp. 162–167.

[17]Koontz, S. L., King, G., Dunnet, A., Kirkendahl, T., Linton, R., and Vaughn, J., "The ISAC Atomic Oxygen Flight Experiment," *Journal of Spacecraft and Rockets*, Vol. 31, No. 3, 1994, pp. 475–488.

[18]Hunton, D. E., Trzcinski, E., Wlodyka, L., Federico, G., and Dorian, J., "Quadrupole Ion/Neutral Mass Spectrometer (for Space Shuttle Applications)," Air Force Geophysics Lab., AFGL-TR-86-0084, Hanscomb AFB, MA, April 1987.

[19]Chen, P., and Straka, S. A., Goddard Space Flight Center, private communication to Steve Koontz.

[20]Linton, R. C., Vaughn, J. A., Fincknor, M. M., Kamenetzky, R. R., DeHaye, R. F., and Whitaker, A. F., "Orbital Atomic Oxygen Effects on Materials: An Overview of MSFC Experiments on the STS-46 EOIM-3," AIAA Paper 93-4102, Sept. 1993.

T. C. Lin
Associate Editor